ARTICLES

An assembly landscape for the 30S ribosomal subunit

Megan W. T. Talkington[1]†, Gary Siuzdak[1] & James R. Williamson[1]

Self-assembling macromolecular machines drive fundamental cellular processes, including transcription, messenger RNA processing, translation, DNA replication and cellular transport. The ribosome, which carries out protein synthesis, is one such machine, and the 30S subunit of the bacterial ribosome is the preeminent model system for biophysical analysis of large RNA–protein complexes. Our understanding of 30S assembly is incomplete, owing to the challenges of monitoring the association of many components simultaneously. Here we have developed a method involving pulse–chase monitored by quantitative mass spectrometry (PC/QMS) to follow the assembly of the 20 ribosomal proteins with 16S ribosomal RNA during formation of the functional particle. These data represent a detailed and quantitative kinetic characterization of the assembly of a large multicomponent macromolecular complex. By measuring the protein binding rates at a range of temperatures, we find that local transformations throughout the assembling subunit have similar but distinct activation energies. Thus, the prevailing view of 30S assembly as a pathway proceeding through a global rate-limiting conformational change must give way to one in which the assembly of the complex traverses a landscape dotted with various local conformational transitions.

The assembly of the 30S ribosomal subunit is a complex dance of macromolecular folding and binding in which 20 proteins bind to rRNA as it folds, creating a complete particle[1–3] that is competent to participate in translation of mRNA. Assembly *in vitro* has shown that secondary structure in the 16S rRNA (local helices) is stabilized by Mg^{2+}-containing buffer alone, but tertiary (long-range) folding depends on the proteins[4]. Because protein binding sites are created as the rRNA folds, ribosomal protein binding reports on local rRNA tertiary conformation throughout assembly[5–9]. Much knowledge of the order and mechanism of 30S assembly has thus been amassed by identifying the proteins bound at equilibrium in incomplete assembly reactions[10,11].

A slow rate-limiting folding transition has long been inferred from the observation that incomplete particles with an altered sedimentation coefficient (21 S versus 30 S) form at low temperatures (0–15 °C; refs 12–14). Heating these incomplete particles, termed the reconstitution intermediate (RI), shifts their sedimentation coefficient to 26 S (RI*) and enables them to complete assembly at low temperatures. The RI → RI* transition, which was thought to be a conformational change in the rRNA, was proposed to be the rate-limiting step of assembly even at higher temperatures, because the apparent concentration independence of the overall assembly rate suggested a unimolecular rate-limiting step[12]. The RI → RI* transition characterizes the canonical scheme of 30S assembly, which has remained essentially unchanged for 35 years:

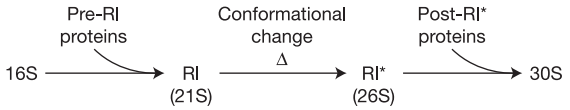

The next step in characterizing the mechanism of 30S assembly is to determine the kinetics by which the various proteins bind to the assembling subunit. Because standard methods are not capable of directly monitoring the binding of many proteins simultaneously, however, we have developed a method, PC/QMS (pulse–chase monitored by quantitative mass spectrometry), that measures the kinetics of binding the individual proteins during assembly of the whole complex.

A method for studying assembly of the whole 30S subunit

PC/QMS takes advantage of the ability of mass spectrometry to quantify large numbers of proteins relative to stable isotope-labelled species, an approach that is widely used in proteomics[15–18]. Assembly of 30S subunits is initiated by incubating the *Escherichia coli* 16S rRNA of 1,542 nucleotides with a mixture of uniformly ^{15}N-labelled 30S proteins (S2–S21)[19]. At various time points, binding of the ^{15}N-proteins is chased with an excess of unlabelled (^{14}N) proteins. Completely formed 30S subunits are purified, and the $^{15}N/^{14}N$ ratio for each protein is determined by matrix-assisted laser-desorption/ionization time-of-flight mass spectrometry (MALDI-TOF[20–22]; Fig. 1a). The $^{15}N/^{14}N$ ratios can be quantified accurately, as judged by standard curves collected on known mixtures of labelled and unlabelled proteins (Fig. 1b), and most of the 30S proteins are observed in a single scan (Fig. 1c). The assay has been validated by measuring the binding rate of the *Aquifex aeolicus* S15 protein to a 16S rRNA fragment using PC/QMS and comparing the results with those of a gel mobility shift assay (see Supplementary Information and Fig. S1). Plotting the fractional isotope ratios for a given protein as a function of time produces a progress curve for the binding of that protein during assembly of the whole subunit. In this way, the binding kinetics of all of the ribosomal proteins can be determined in a single experiment.

Protein binding rates match the existing 30S assembly map

Under standard conditions (see Methods), similar to those identified as optimal for *in vitro* assembly[12], the proteins bind with rates distributed throughout two orders of magnitude (Fig. 2a–c). The trends in these data correspond well to protein binding rates inferred

[1]Departments of Molecular Biology and Chemistry, and The Skaggs Institute for Chemical Biology, The Scripps Research Institute, La Jolla, California 92037, USA. †Present address: Department of Microbiology and Molecular Genetics, Harvard Medical School, Boston, Massachusetts 02115, USA.

from the reactivity of 16S rRNA nucleotides to chemical probes over time[6] and to the binding order determined in classical equilibrium experiments[10] (Fig. 2b). Assembly *in vitro* maintains the 5′ to 3′ directionality and overall protein binding order, including late assembly of the interdomain junction that forms the site of mRNA decoding (Fig. 2c), that is observed *in vivo*[6,23], despite taking place on a mature 16S rRNA rather than on a nascent precursor rRNA transcript[24,25].

Folding and binding occur at similar rates

Characterizing the mechanism of 30S assembly requires measurement of the protein binding kinetics under various conditions, and PC/QMS is sufficiently rapid to permit the collection of data sets in several different conditions. To begin probing the nature of the rate-limiting steps of assembly, we varied the concentration of rRNA and proteins in the assembly reaction. At one extreme, if binding is the rate-limiting step for a particular protein, then the binding rate should be directly proportional to the concentration. At the other extreme, if a unimolecular folding event is rate-limiting, then the rate should be insensitive to concentration. In fact, the intermediate situation is observed for many proteins—that is, the protein binding rates are weakly affected by concentration (Fig. 3)—which indicates that RNA folding and protein binding occur at similar rates. All of the proteins observed here show some concentration dependence in their binding rates; thus, folding does not seem to be rate-limiting for any of them.

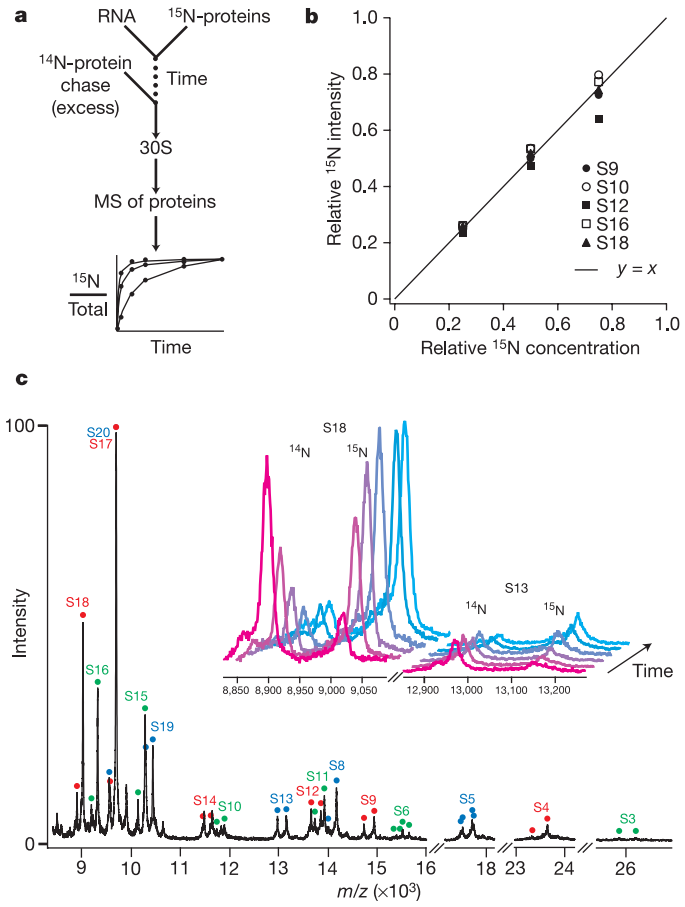

Figure 1 | The PC/QMS method for measuring protein binding kinetics in the 30S ribosomal subunit. a, The PC/QMS method. **b**, Quantification of relative ^{15}N-protein concentrations for several proteins from three standard mixtures of native ^{15}N- and ^{14}N-30S subunits. The average relative intensities for all proteins from the three mixtures were 0.24 ± 0.03, 0.50 ± 0.03 and 0.73 ± 0.04 (mean ± s.d.). **c**, MALDI-TOF mass spectrum of 30S proteins from the 2-min time point of an assembly reaction done under standard conditions. Inset shows expanded spectra for several time points for proteins S18 and S13. Additional details are provided in the Supplementary Information.

30S assembly proceeds through many rate-limiting transitions

To characterize assembly intermediates, we measured protein binding rates at low temperature, where RI has been found to accumulate. The ^{15}N-protein pulse was done at low temperature, and the temperature was restored to the optimum (40 °C) upon addition of the ^{14}N-protein chase. Consistent with previous measurements of overall assembly rates[12], protein binding is slow at 15 °C (Fig. 4a), requiring more than 2 days to proceed to completion. Unexpectedly, none of the proteins is disproportionately slowed as compared with the others and none plateaus at a low extent of binding—an observation that initially seems to be inconsistent with stalling of assembly at a 21S intermediate (RI).

The standard RI ⟶ RI* mechanism, whereby assembly stalls at the 21S intermediate at low temperatures, implies that the late proteins have much lower rates of binding than the early proteins at low temperatures, whereas the binding rates for all proteins are more similar at 40 °C, where assembly proceeds smoothly. The temperature dependence of the protein binding rates is characterized by the Arrhenius activation energy (E_a), and there are generally two ways to explain the previous observations in terms of activation energies. Either the activation energies are much larger for the late binding proteins than for the early binding proteins, or there is a change in the rate-determining step for the late proteins to a process with a larger activation energy at low temperatures.

The temperature dependence of the binding rate of each protein was measured over the accessible range (Fig. 4b), and the activation energies were determined from the slopes of the Arrhenius plots (Fig. 4b, c). The activation energies are generally similar for all of the proteins, being scattered throughout a relatively narrow range of ~24–44 kcal mol^{-1}. The binding activation energies observed are all similar to the E_a for overall assembly of 38 kcal mol^{-1} determined previously (ref. 12). The magnitude of the activation energies corresponds to the melting of about four RNA base pairs[26] and also corresponds to the activation energy for the folding of small proteins, although we cannot at present determine the relative contributions of RNA and protein folding to the kinetics observed. Although there is a rough trend that the activation energies are slightly larger for the late binding proteins than for the early binding proteins, the correlation is poor, and the magnitude of the differences in activation energy is insufficient to produce stalling of assembly at low temperature. Furthermore, the Arrhenius plots are linear over the accessible range (see Methods), which clearly indicates that the activation energies do not change with temperature and thus that the rate-determining step is the same for each protein at high and low temperature.

Consequently, no one step is solely responsible for the apparent E_a of overall assembly. The slowly binding proteins, which include both those that precede the canonical RI ⟶ RI* transition and those that follow it, do not have the highest E_a values (Fig. 4c), so the last steps of assembly are not more dependent on temperature than the earlier steps. Furthermore, the rates and E_a values of the slowly binding proteins are not well correlated, indicating that the final stages of assembly are limited by many different transitions. Until now, there has been no way to follow these different transitions because the individual protein binding rates have not been determined during assembly at several temperatures. PC/QMS has enabled us to do this, and we find that the classic RI ⟶ RI* mechanism is not adequate to explain the rates and activation energies observed for binding of the individual proteins.

These observations suggest that although a 21S 'particle' can be isolated from assembly at low temperature, this 21S particle is not a true assembly 'intermediate'. It seems likely that the reason that 21S particles are retrieved from sucrose gradient purification of

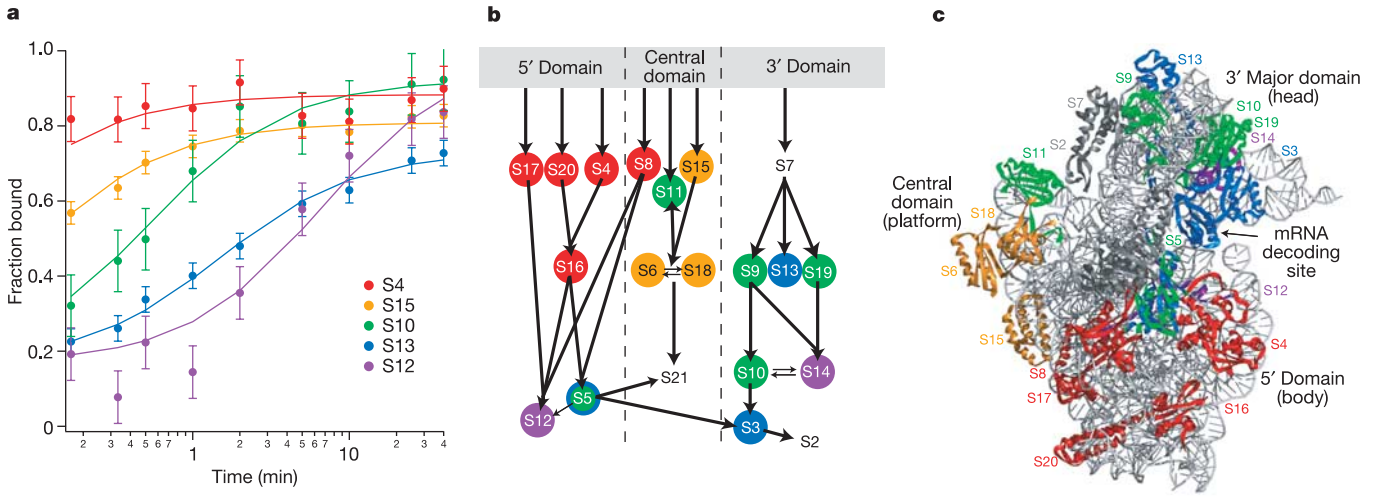

Figure 2 | Binding kinetics of 30S proteins measured using PC/QMS under standard conditions. **a**, Representative progress curves for protein binding (see Supplementary Fig. S2), fitted as described in the Methods. The error bars are derived from the s.d. of standard samples (see Supplementary Information). **b**, Proteins in the Nomura assembly map (refs 10, 11; and S. C. Agalarov & J.R.W., unpublished data) are coloured by their binding rates (see Supplementary Table S1). Red, 20 to $\geq$30 min^{-1}; orange, 8.1–15 min^{-1}; green, 1.2–2.2 min^{-1}; blue, 0.38–0.73 min^{-1}; purple, 0.18–0.26 min^{-1}. S5 is shown in green and blue to represent the binding rates of the unacetylated and acetylated forms, respectively. Grey bar represents 16S rRNA. **c**, Proteins in an X-ray crystal structure of the 30S subunit from *T. thermophilus*[1], coloured as in **b**.

low-temperature assembly reactions is that a diverse collection of unstable particles that are in the process of assembling all sediment at ~21 S until they accomplish a transition that shifts them to 26 S. This depiction agrees with the previous observations that the characteristics of RI are variable and that some pre-RI proteins bind only transiently at the RI stage[13]. It is likely that weakly bound proteins dissociate to different extents during the PC/QMS chase as compared with sucrose gradient centrifugation, such that the binding of some 'pre-RI' proteins (particularly S5, S12 and S19) is observed to be slow by PC/QMS.

The slight clustering in protein binding rates at 15 °C (Fig. 4a, c) may indicate the presence of populated assembly intermediates. Because the members of a group do not share the same activation energy (Fig. 4c), however, it seems that the binding of the proteins in a given group are not all limited by a single RNA folding step. Assembly by various local transitions rather than a single, global step enables the various subunits in a population to assemble into the native structure by various routes rather than a requisite pathway. Equilibrium footprinting of reconstituted RI and RI* particles indicates that conformational changes are scattered throughout the 16S rRNA sequence, although centred on the active site[14]. This observation is consistent with the presence of many local conformational changes that may take place in parallel during late stages of assembly. Thus, just as macromolecular folding pathways have been expanded to folding landscapes that can be traversed by any of various parallel pathways[27–30], so too can the assembly of a multicomponent complex, the 30S subunit, now be represented by a landscape (Fig. 5).

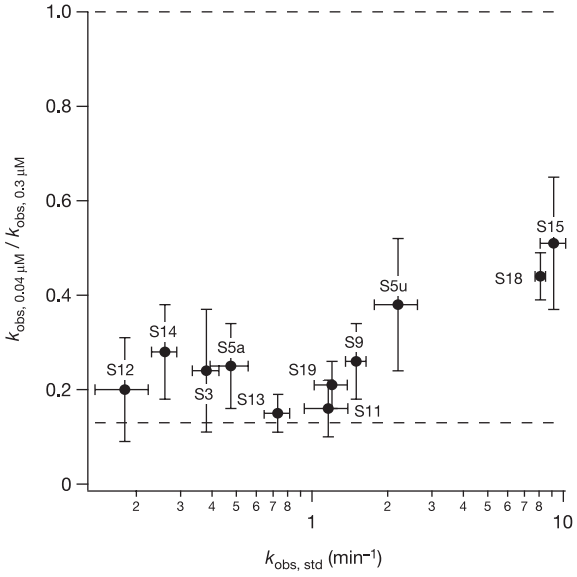

Figure 3 | Ratio of the protein binding rates observed at two concentrations versus the rates at standard concentration. Ratios of 1.0 or 0.13 (broken lines) would indicate unimolecular or bimolecular rate-limiting steps, respectively. The errors in k_{obs} (s.d. from the fits of progress curves) are propagated to produce the errors bars. Proteins that bind very rapidly at the standard concentration are not shown, because the rates cannot be accurately determined from the present data. S10 data are not shown owing to a poor signal. Proteins S6 and S8 have high ratios, similar to two other central domain proteins, S18 and S15. Proteins S16, S17 and S20 have lower ratios, similar to most proteins.

An assembly landscape for the 30S subunit

In the landscape representation all possible conformations of the 16S rRNA map onto a free-energy surface, but in the absence of proteins the native 30S conformation is energetically unfavourable. Folding can proceed along many possible pathways to the native state because the landscape is composed of many local and modest barriers. A unique feature of the 30S landscape, as compared with unimolecular folding landscapes[27], is the intermolecular protein binding, which alters the shape of the free-energy surface during the assembly process. Once RNA folding produces a new binding site, protein binding creates new downhill directions by which further RNA folding can proceed. The marked alteration of the 16S folding landscape that accompanies ribosomal protein binding is analogous to the changes in protein folding landscapes that occur on shifting from denaturing to native conditions. Each protein binding event further stabilizes the native 30S conformation until all assembly pathways converge at this state. Despite the changes in the landscape that accompany protein binding, the heights of the various barriers encountered on any particular pathway seem to be similar.

Viewing 30S assembly as a landscape is supported not only by the

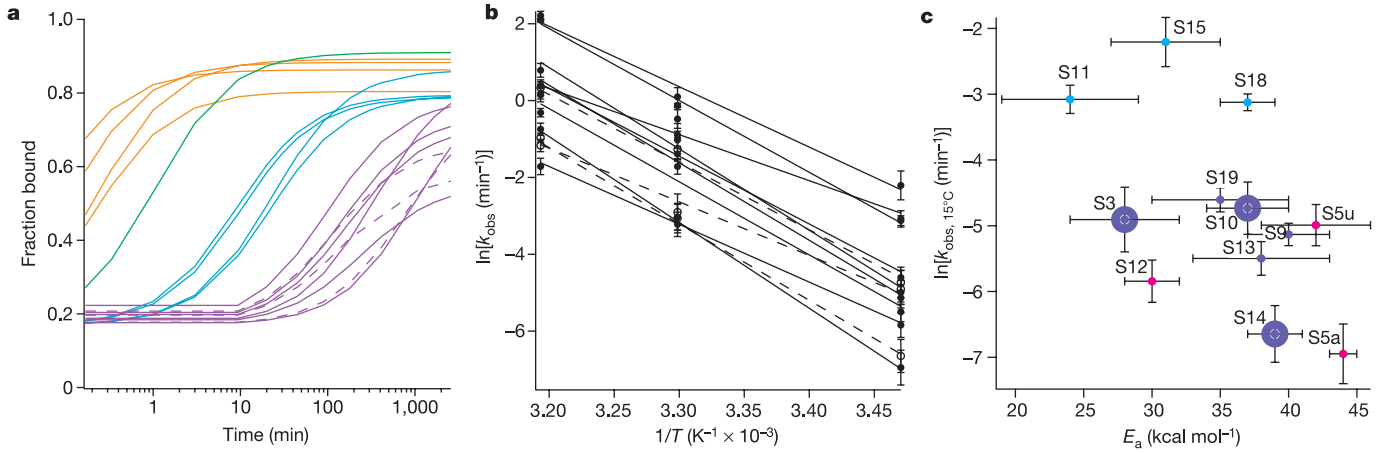

Figure 4 | The temperature dependence of protein binding rates. **a**, Fits of binding progress curves at 15 °C, coloured according to the rates (see Supplementary Table S1). Orange, 4.4–21 min^{-1}; green, 1.0 min^{-1}; cyan, 0.044–0.11 min^{-1}; purple, 0.00096–0.010 min^{-1}. Post-RI* proteins (S3, S10 and S14) are shown as broken lines here and in **b**. **b**, Arrhenius plots of the observed rates (see Supplementary Fig. S3). The errors in k_{obs} (s.d. from the fits of progress curves) are propagated to produce the error bars. Proteins that bind very rapidly are not shown here or in **c**. **c**, Protein binding rates at 15 °C versus the activation energies (see Supplementary Table S1). The errors in E_a are the s.d. from the linear Arrhenius plot fits. Proteins are coloured according to the 30S domain (magenta, 5′ domain; cyan, central domain; purple, 3′ domain). Post-RI* proteins have large points.

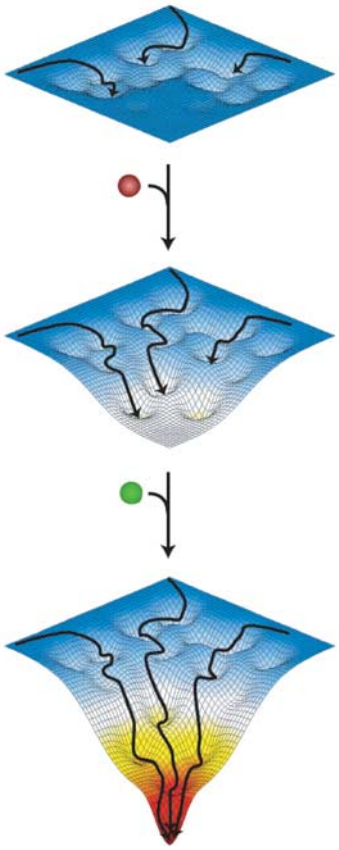

Figure 5 | An assembly landscape for 30S assembly. The horizontal axes of the surface correspond to 16S rRNA conformational space, and the vertical axis is free energy. The native conformation of the 16S rRNA adopted in the 30S subunit is located at the bottom corner. In the absence of proteins, this is not the lowest-energy conformation of the RNA. Parallel folding pathways are indicated by the arrows on the energy surface. Local folding creates protein binding sites, and large changes in the landscape accompany protein binding (coloured spheres). Sequential protein binding eventually stabilizes the native 30S conformation. All pathways converge on this point, and there is no bottleneck through which all folding trajectories must pass.

detailed kinetic data reported here, but also by the classical equilibrium data summarized in the assembly map (Fig. 2b), which show that the ribosomal proteins do not have an absolute dependence on each other for binding, but rather can bind in various orders[31]. Indeed, Nomura and colleagues predicted that assembly actually proceeds by several pathways even as they proposed the simple RI ⟶ RI* model, because it was observed that different proteins potentiated the formation of RI* particles to varying extents[13].

Assembly by a global rate-limiting step, which would be represented by a bottleneck on the landscape, could bring assembly to a standstill under non-optimal conditions. Assembly through a landscape of different barriers, by contrast, would mean that slowing any one of the steps would slow down, but not completely stall, assembly. Such a robust assembly landscape is surely one of many functions encoded by strongly conserved ribosomal sequences. RNA and protein chaperones are expected to have a role in assembly, and the protein chaperone DnaK has been specifically implicated in aiding 30S assembly[32–34]. The landscape model developed here predicts that there are many folding transitions that are points at which chaperones might assist.

The assay introduced here, PC/QMS, has made it possible to begin to construct an assembly landscape for a large macromolecular complex, the 30S ribosomal subunit. The assay reports the kinetics at which different sites throughout the 30S subunit assemble, and it can be conducted under various conditions designed to mimic the intracellular assembly reaction, as well as with 30S components engineered to assess the roles of particular components and functional groups. We expect that themes from the 30S assembly landscape will inform our understanding of the assembly of ribonucleoproteins and of large complexes in general. As a general method suitable for studying site-specific assembly in multicomponent complexes, PC/QMS can also be adapted to these systems.

METHODS

Pulse–chase assembly of 30S subunits. Mixtures of all 30S proteins (unlabelled or ^{15}N-labelled) and 16S rRNA were prepared from native 30S subunits (see Supplementary Information). Binding titrations indicated that the concentrations of active proteins in the mixtures were roughly stoichiometric (within ~2-fold); thus, differences in the concentrations of the proteins should have a minimal effect on the binding rates observed. The standard assembly conditions were 0.3 μM 16S and 0.45 μM ^{15}N-proteins in assembly buffer containing 25 mM Tris-HCl (pH 7.5 at room temperature), 330 mM KCl, 20 mM $MgCl_2$ and 2 mM dithiothreitol at 40 °C (ref. 35); the chase was 5 × unlabelled proteins. Non-specific binding of the excess proteins in the chase was resolved by purifying the

assembled 30S subunits in 10–40% sucrose gradients containing a high salt concentration (assembly buffer plus 0.5 M NH_4Cl). Particles assembled under standard conditions in the presence of excess proteins and purified in high-salt conditions are properly formed, as judged by the extent to which they bind 50S subunits to form particles that migrate as 70S particles[36]. (Assembled subunits are slightly less active than native 30S; assembled and chased subunits are as active as those that are not chased.)

The PC/QMS assay was done at 40, 30 and 15 °C. The very low rate of assembly at low temperatures makes 15 °C the lowest temperature at which it is practical to measure binding kinetics; over the course of a 6-d experiment at 10 °C, some precipitation was observed in protein samples, causing concerns about the integrity of samples over the long periods of time required for assembly at such low temperatures (see Supplementary Table S1).

MALDI analysis. The proteins bound during the pulse–chase reaction were extracted from the assembled 30S subunits (see Supplementary Information). The extracted proteins were analysed with a Voyager-DE STR MALDI-TOF mass spectrometer (PerSeptive Biosystems) operated in linear mode. The intensities of the protein peaks were determined by fitting each peak to a single gaussian function using Igor Pro (WaveMetrics). The heights of the gaussian fits (after background subtraction; see Supplementary Information) were taken as the peak intensities. We report the relative ^{15}N-labelled protein intensities: ^{15}N-protein/(^{14}N-protein + ^{15}N-protein).

Analysis of protein binding progress curves. The progress curves of relative ^{15}N-protein intensity versus time were fitted to an equation of two-state binding for a bimolecular system, R + P → RP:

$$d[RP]/dt = k_{on}[R][P] - k_{off}[RP]$$

where R is 16S rRNA, P is one of the proteins, and RP is the complex. Because ^{15}N-protein binding was chased with 5 × ^{14}N-proteins, the minimum fraction of ^{15}N-protein bound was 0.17 (1/(1 + 5) = 0.17). The binding rate observed is the product of k_{on} and the total RNA concentration ($k_{obs} = k_{on}[R_T]$). For most proteins, this observed binding rate probably represents many rate constants—binding of the protein itself as well as earlier proteins and rRNA folding.

Arrhenius analysis. The activation energies of protein binding are calculated from the slopes of the Arrhenius plots using the Arrhenius equation, $k = Ae^{-E_a/RT}$.

Received 14 July; accepted 22 September 2005.

1. Wimberly, B. T. *et al.* Structure of the 30S ribosomal subunit. *Nature* **407,** 327–339 (2000).
2. Schluenzen, F. *et al.* Structure of functionally activated small ribosomal subunit at 3.3 Å resolution. *Cell* **102,** 615–623 (2000).
3. Brodersen, D. E., Clemons, W. M. Jr, Carter, A. P., Wimberly, B. T. & Ramakrishnan, V. Crystal structure of the 30 S ribosomal subunit from *Thermus thermophilus*: structure of the proteins and their interactions with 16 S RNA. *J. Mol. Biol.* **316,** 725–768 (2002).
4. Moazed, D., Stern, S. & Noller, H. F. Rapid chemical probing of conformation in 16 S ribosomal RNA and 30 S ribosomal subunits using primer extension. *J. Mol. Biol.* **187,** 399–416 (1986).
5. Agalarov, S. C. & Williamson, J. R. A hierarchy of RNA subdomains in assembly of the central domain of the 30 S ribosomal subunit. *RNA* **6,** 402–408 (2000).
6. Powers, T., Daubresse, G. & Noller, H. F. Dynamics of *in vitro* assembly of 16 S rRNA into 30 S ribosomal subunits. *J. Mol. Biol.* **232,** 362–374 (1993).
7. Recht, M. I. & Williamson, J. R. Thermodynamics and kinetics of central domain assembly. *Cold Spring Harbor Symp. Quant. Biol.* **66,** 591–598 (2001).
8. Stagg, S. M., Mears, J. A. & Harvey, S. C. A structural model for the assembly of the 30S subunit of the ribosome. *J. Mol. Biol.* **328,** 49–61 (2003).
9. Stern, S., Powers, T., Changchien, L. M. & Noller, H. F. RNA–protein interactions in 30S ribosomal subunits: folding and function of 16S rRNA. *Science* **244,** 783–790 (1989).
10. Held, W. A., Ballou, B., Mizushima, S. & Nomura, M. Assembly mapping of 30 S ribosomal proteins from *Escherichia coli*. *J. Biol. Chem.* **249,** 3103–3111 (1974).
11. Culver, G. M. Assembly of the 30S ribosomal subunit. *Biopolymers* **68,** 234–249 (2003).
12. Traub, P. & Nomura, M. Structure and function of *Escherichia coli* ribosomes VI. Mechanism of assembly of 30 S ribosomes studied *in vitro*. *J. Mol. Biol.* **40,** 391–413 (1969).
13. Held, W. A. & Nomura, M. Rate-determining step in the reconstitution of *Escherichia coli* 30S ribosomal subunits. *Biochemistry* **12,** 3273–3281 (1973).
14. Holmes, K. L. & Culver, G. M. Mapping structural differences between 30S ribosomal subunit assembly intermediates. *Nature Struct. Mol. Biol.* **11,** 179–186 (2004).
15. Gygi, S. P. *et al.* Quantitative analysis of complex protein mixtures using isotope-coded affinity tags. *Nature Biotechnol.* **17,** 994–999 (1999).
16. Oda, Y., Huang, K., Cross, F. R., Cowburn, D. & Chait, B. T. Accurate quantitation of protein expression and site-specific phosphorylation. *Proc. Natl Acad. Sci. USA* **96,** 6591–6596 (1999).
17. Pasa-Tolic, L. *et al.* High throughput proteome-wide precision measurements of protein expression using mass spectrometry. *J. Am. Chem. Soc.* **121,** 7949–7950 (1999).
18. Sechi, S. & Oda, Y. Quantitative proteomics using mass spectrometry. *Curr. Opin. Chem. Biol.* **7,** 70–77 (2003).
19. Traub, P. & Nomura, M. Structure and function of *E. coli* ribosomes. V. Reconstitution of functionally active 30S ribosomal particles from RNA and proteins. *Proc. Natl Acad. Sci. USA* **59,** 777–784 (1968).
20. Beavis, R. C. & Chait, B. T. Matrix-assisted laser desorption ionization mass-spectrometry of proteins. *Methods Enzymol.* **270,** 519–551 (1996).
21. Hillenkamp, F. & Karas, M. Mass spectrometry of peptides and proteins by matrix-assisted ultraviolet laser desorption/ionization. *Methods Enzymol.* **193,** 280–295 (1990).
22. Jennings, K. R. & Dolnikowski, G. G. Mass analyzers. *Methods Enzymol.* **193,** 37–61 (1990).
23. Pichon, J., Marvaldi, J. & Marchis-Mouren, G. The *in vivo* order of protein addition in the course of *Escherichia coli* 30 S and 50 S subunit biogenesis. *J. Mol. Biol.* **96,** 125–137 (1975).
24. Mangiarotti, G., Apirion, D., Schlessinger, D. & Silengo, L. Biosynthetic precursors of 30S and 50S ribosomal particles in *Escherichia coli*. *Biochemistry* **7,** 456–472 (1968).
25. Srivastava, A. K. & Schlessinger, D. in *The Ribosome: Structure, Function, & Evolution* (ed. Hill, W. *et al.*) 426–434 (American Society of Microbiology, Washington DC, 1990).
26. Xia, T. *et al.* Thermodynamic parameters for an expanded nearest-neighbour model for formation of RNA duplexes with Watson–Crick base pairs. *Biochemistry* **37,** 14719–14735 (1998).
27. Dill, K. A. & Chan, H. S. From Levinthal to pathways to funnels. *Nature Struct. Biol.* **4,** 10–19 (1997).
28. Pan, J., Thirumalai, D. & Woodson, S. A. Folding of RNA involves parallel pathways. *J. Mol. Biol.* **273,** 7–13 (1997).
29. Rook, M. S., Treiber, D. K. & Williamson, J. R. Fast folding mutants of the *Tetrahymena* group I ribozyme reveal a rugged folding energy landscape. *J. Mol. Biol.* **281,** 609–620 (1998).
30. Thirumalai, D. & Woodson, S. A. Kinetics of folding of proteins and RNA. *Acc. Chem. Res.* **29,** 433–439 (1996).
31. Nomura, M. Assembly of bacterial ribosomes. *Science* **179,** 864–873 (1973).
32. Alix, J. H. & Guerin, M. F. Mutant DnaK chaperones cause ribosome assembly defects in *Escherichia coli*. *Proc. Natl Acad. Sci. USA* **90,** 9725–9729 (1993).
33. Maki, J. A., Schnobrich, D. J. & Culver, G. M. The DnaK chaperone system facilitates 30S ribosomal subunit assembly. *Mol. Cell* **10,** 129–138 (2002).
34. Maki, J. A., Southworth, D. R. & Culver, G. M. Demonstration of the role of the DnaK chaperone system in assembly of 30S ribosomal subunits using a purified *in vitro* system. *RNA* **9,** 1418–1421 (2003).
35. Serdyuk, I. N., Agalarov, S. C., Sedelnikova, S. E., Spirin, A. S. & May, R. P. Shape and compactness of the isolated ribosomal 16 S RNA and its complexes with ribosomal proteins. *J. Mol. Biol.* **169,** 409–425 (1983).
36. Culver, G. M. & Noller, H. F. Efficient reconstitution of functional *Escherichia coli* 30S ribosomal subunits from a complete set of recombinant small subunit ribosomal proteins. *RNA* **5,** 832–843 (1999).

Supplementary Information is linked to the online version of the paper at www.nature.com/nature.

Acknowledgements We thank the staff of the TSRI Center for Mass Spectrometry for assistance with mass spectrometry; M. I. Recht, S. C. Agalarov and S. P. Ryder for discussions and technical assistance; the laboratories of D. B. Goodin, S. P. Mayfield and A. Schneemann for use of equipment; and M. J. Fedor, J. D. Puglisi and S. P. Ryder for critically reading the manuscript. This work was supported by a grant from the NIH (to J.R.W.) and by predoctoral fellowships from the NSF and the Skaggs Institute for Chemical Biology (to M.W.T.T.).

Author Contributions The experimental work in this manuscript was carried out by M.W.T.T., with advice and support from G.S. and J.R.W.

Author Information Reprints and permissions information is available at npg.nature.com/reprintsandpermissions. The authors declare no competing financial interests. Correspondence and requests for materials should be addressed to J.R.W. (jrwill@scripps.edu).